Fine Structure of the $1s3p\ ^3P_J$ Level in Atomic ^{4}He: Theory and Experiment

P. Mueller,[1,*] L.-B. Wang,[1,2] G. W. F. Drake,[3,†] K. Bailey,[1] Z.-T. Lu,[1,4] and T. P. O'Connor[1]

[1]*Physics Division, Argonne National Laboratory, Argonne, Illinois 60439, USA*
[2]*Physics Department, University of Illinois at Urbana-Champaign, Urbana, Illinois 61801, USA*
[3]*Physics Department, University of Windsor, Windsor, Ontario, Canada N9B 3P4*
[4]*The Enrico Fermi Institute and Department of Physics, The University of Chicago, Chicago, Illinois 60637, USA*
(Received 22 July 2004; published 7 April 2005)

The fine structure intervals in helium have been the focus of many theoretical and experimental studies in recent years with most of them concentrating on the $1s2p\ ^3P_J$ levels. Here, we report on a theoretical calculation and an experimental determination of the $1s2p\ ^3P_J$ fine structure intervals. The values from the theoretical calculation are 8113.730(6) and 658.801(6) MHz for the ν_{01} and ν_{12} intervals, respectively. The laser spectroscopic measurement reported here yields 8113.714(28) and 658.810(18) MHz for these intervals and is in excellent agreement with the theoretical calculation. Both, however, disagree significantly with the previous most precise experimental results.

The fine structure intervals in helium have attracted a great deal of interest in recent years because of the possibility of using a comparison between theory [1,2] and experiment [3–5] to better determine the fine structure constant $\alpha = e^2/\hbar c$. For example, for the $1s2p\ ^3P_J$ state of helium ($J = 0, 1, 2$), a measurement of the large interval $\nu_{01} \simeq 29\,617$ MHz to an accuracy of ± 1 kHz is sufficient to determine α with an accuracy of ± 16 ppb (parts per 10^9).

In comparison to the $1s2p\ ^3P_J$ level the available data on the fine structure splitting of $1s3p\ ^3P_J$ is relatively limited. The work by Yang *et al.* [6] stands out as the only experiment that has reached a precision of better than 100 kHz for all $1s3p\ ^3P_J$ fine structure intervals. Additionally, no theoretical work has been published so far to follow up on these results at the same precision level. There are more recent experimental results from high resolution laser spectroscopy on the $1s2s\ ^3S_1 \rightarrow 1s3p\ ^3P_J$ transitions. However, these experiments concentrated on the measurement of the ^{3}He-^{4}He isotope shift [7] and on the absolute transition frequency [8,9].

As will be shown, the theoretical values for the $1s3p\ ^3P_J$ state published here disagree by about 250 kHz with the results from [6]. This discrepancy is particularly troubling since all the higher-order corrections, which in principle might be responsible for the discrepancy if they were incorrect, decrease roughly in proportion to $1/n^3$, where n is the principal quantum number. Consequently, they are smaller by a factor of $(2/3)^3 \simeq 0.3$ than in the $1s2p\ ^3P_J$ state. In this Letter we present the theoretical calculation of the $1s3p\ ^3P_J$ fine structure splittings along with a more accurate measurement of these intervals to address the apparent discrepancy.

To a first approximation, the various theoretical contributions to the fine structure splittings come from the spin-orbit (so), spin-other-orbit (soo), and spin-spin (ss) terms of order α^2 Ry in the Breit-Pauli interaction. However, comparisons with experiment at the level of a few kHz

also require the calculation of higher-order corrections of order α^3, α^4, $\alpha^5 \ln\alpha$, and α^5. The complete expression for the spin-dependent energy shift up to this order is then of the form [1]

$$\Delta E_J = \alpha^2 \langle B_{2,0} \rangle + \alpha^3 \langle B_{3,0} \rangle + \alpha^4 \langle B_{2,0} G' B_{2,0} \rangle + \alpha^4 \langle B_{4,0} \rangle$$
$$+ \alpha^5 \ln(Z\alpha)^{-2} \langle B_{5,1}^{so} \rangle + 2\alpha^5 \ln(Z\alpha)^{-2} \langle B_{2,0} G' A_{3,1} \rangle$$
$$+ \alpha^5 \ln\alpha \langle B_{5,1}^{soo} + B_{5,1}^{ss} \rangle + \alpha^5 \langle B_{5,0} \rangle$$
$$+ 2\alpha^5 \langle B_{2,0} G' A_{3,0} \rangle + O(\alpha^6) \qquad (1)$$

where $A_{m,n}$ and $B_{m,n}$ stand for combinations of relativistic and QED operators multiplying terms proportional to $\alpha^m (\ln\alpha)^n$ and G' denotes the reduced Green's function for second-order contributions. The leading term $B_{2,0}$ is the standard Breit-Pauli interaction. $B_{3,0}$ comes from the anomalous magnetic moment, and $B_{4,0}$ contains the sum of 15 Douglas-Kroll operators [10]. The terms $B_{5,1}$ and $B_{5,0}$ are quantum electrodynamic corrections first derived by Zhang [11]. The $B_{5,1}$ part has been independently verified by Pachucki and Sapirstein [2]. However, the term $B_{5,0}$ presents significant theoretical challenges, and it has only partially received independent verification. Fortunately, this term is small enough to be neglected for the purposes of this work. In addition, there are finite mass corrections to each of the above terms involving an additional factor of μ/M or $(\mu/M)^2$ which must be taken into account, where μ/M is the ratio of the reduced electron mass to the nuclear mass.

As discussed previously [1], the principal computational step is the calculation of the matrix elements of the various operators in Eq. (1) with respect to high precision variational wave functions, and the evaluation of the second-order terms. The results for the terms up to and including order $\alpha^5 \ln\alpha$, and the finite mass corrections up to order $\alpha^3 \mu/M$, are displayed in Table I. The omitted terms of order α^5 and $\alpha^4 \mu/M$ are known in the case of the $1s2p\ ^3P_J$ state of helium to give a net contribution of

TABLE I. Summary of contributions to the fine structure intervals of the $1s3p\,^3P_J$ levels in helium. Units are MHz.

| Term	ν_{01}	ν_{12}
$\alpha^2\langle B_{2,0}\rangle$	8099.8771	666.1254
$\alpha^2(\mu/M)\delta_M\langle B_{2,0}\rangle$	-0.7754	0.8131
$\alpha^2(\mu/M)^2\delta_M^{(2)}\langle B_{2,0}\rangle$	0.0000	-0.0001
$\alpha^3\langle B_{3,0}\rangle$	14.8273	-6.4273
$\alpha^3(\mu/M)\delta_M\langle B_{3,0}\rangle$	-0.0020	0.0014
$\alpha^4\langle B_{4,0}\rangle$	-0.9654	0.5360
$\alpha^4\langle B_{2,0}G'B_{2,0}\rangle$	0.7701(4)	$-2.2369(5)$
$\alpha^5\ln(Z\alpha)^{-2}\langle B_{5,1}^{\mathrm{so}}\rangle$	0.0105	0.0210
$\alpha^5\ln\alpha\langle B_{5,1}^{\mathrm{soo}}\rangle$	-0.0036	-0.0072
$\alpha^5\ln\alpha\langle B_{5,1}^{\mathrm{ss}}\rangle$	0.0063	-0.0025
$\alpha^5\ln(Z\alpha)^{-2}2\langle B_{2,0}G'A_{3,1}\rangle$	-0.0151	-0.0217
|higher order terms|	≤ 0.0060	≤ 0.0060
Total	8113.7297	658.8012

FIG. 1 (color online). Schematic of the experimental setup used for the detection of laser induced fluorescence from a beam of metastable helium atoms.

less than ± 20 kHz. With the $1/n^3$ scaling, this would reduce to ± 6 kHz for the $1s3p\,^3P_J$ state, which is the value we take as an estimate for the uncertainty due to the omitted higher-order terms. This level of accuracy is more than sufficient for comparison with the accuracy of the measurements presented here. However, a full calculation of these terms would be necessary if the experimental accuracy were improved to ± 6 kHz, and a measurement at the ± 1 kHz would provide an important test of theory.

The new experimental determination of the fine structure intervals reported here is based on laser induced fluorescence detection in an atomic beam as shown in Fig. 1 [12]. Metastable helium atoms are produced in a rf driven discharge source that is cooled to liquid nitrogen (LN$_2$) temperature. Two-dimensional transverse cooling on the $1s2s\,^3S_1 \rightarrow 1s2p\,^3P_2$ transition at 1083 nm is used to reduce the divergence of the atomic beam of metastable helium and increase its forward intensity by a factor of 10. After passing a collimator and a flight path of 180 cm the atomic beam is finally overlapped perpendicularly with two antiparallel laser beams at a wavelength of 389 nm to excite the $1s2s\,^3S_1 \rightarrow 1s3p\,^3P_J$ ($J = 0, 1, 2$) transitions. A pair of lenses images the laser induced fluorescence onto a photo-multiplier tube (PMT). The overall efficiency for the photon detection is about 0.1%. The interaction region is enclosed by a magnetic shield with an attenuation factor of 800 to minimize possible effects from Zeeman shifts.

The frequency stability and control of the 389 nm laser light is of key importance for the accurate determination of the fine structure splitting. The 389 nm light is generated through frequency doubling of the amplified output of an external-cavity diode laser (DL1) operating at 778 nm. The frequency of DL1 is locked to a high finesse Fabry-Perot interferometer (FPI). A frequency tunable acousto-optic modulator (AOM) is placed between DL1 and the FPI and works as a frequency shifter to allow for scanning
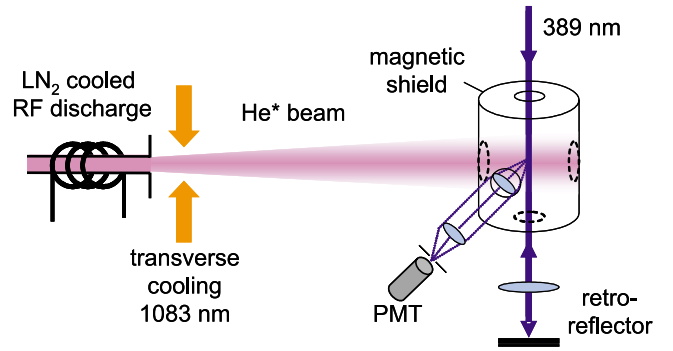
the DL1 frequency relative to a selected FPI mode. To stabilize the absolute frequency positions of the FPI modes, the FPI is locked to a second diode laser at 778 nm (DL2), which is itself referenced to a saturated absorption signal from an iodine cell. The iodine spectrometer provides a long-term frequency stability of better than 15 kHz in 1 min, which translates to a stability of better than 30 kHz in 1 min for the 389 nm light. Partial beams from DL1 and DL2 are overlapped onto a fast photodiode and the resulting beat frequency is amplified and continuously monitored by a microwave frequency counter that is referenced to a rubidium disciplined crystal oscillator with a relative frequency uncertainty of less than 1 ppb.

The blue laser beam is spatially filtered and expanded to a diameter of about 1 cm before being sent through the interaction region. A retroreflector on the opposite side of the vacuum chamber ensures that the counterpropagating laser beam is in exact anticollinear geometry. This arrangement largely cancels possible Doppler shifts that would result from systematic laser beam steering when switching between the different transitions. Additionally, the laser beam is carefully aligned to be exactly perpendicular to the atomic beam by matching the resonance center position obtained with two laser beams to the one obtained when the return beam is blocked. During the experiment, the alignment is constantly checked by monitoring the reverse transmission of the retroreflected beam through the spatial filter pinhole.

To obtain a resonance curve, the blue laser frequency is scanned to cover a range of about ± 15 MHz around the fluorescence maximum by discrete changes of the oscillator frequency that drives the AOM. At each frequency step, the beat frequency and the PMT count rate are recorded as data. Figure 2 shows a typical example of the resonant curve for the $1s2s\,^3S_1 \rightarrow 1s3p\,^3P_J$ transition. The PMT count is plotted as a function of the laser frequency relative to the line center. The errors on the photon counts are not purely statistical, but also include a 3%–5% contribution from the power fluctuation of the blue laser light during the counting gate of 0.5 s. We did not observe any dependence of the power on the laser frequency nor any significant drift
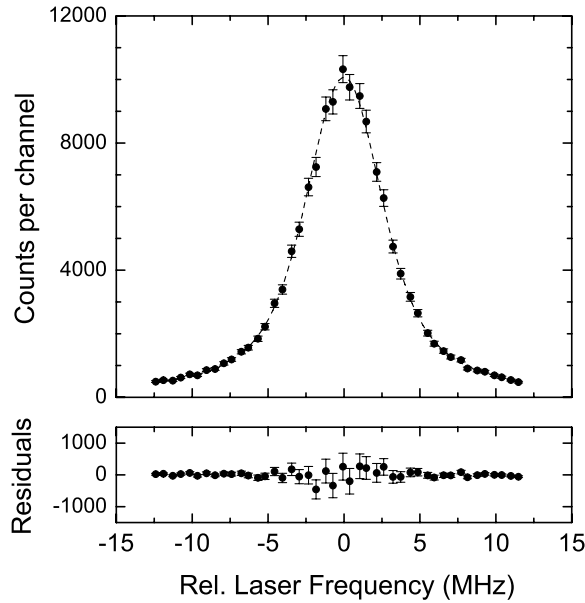
FIG. 2.   Typical resonance profile for the $1s2s\ ^3S_1 \rightarrow 1s3p\ ^3P_2$ transition taken at a laser power of 50 μW. The dashed line is a least-square fit of a Voigt profile to the data. The fit uncertainty on the line center is 23 kHz. The respective residuals are shown in the lower plot.

FIG. 3.   Experimental fine structure splittings for (a) $\nu_{01}(J = 0 \rightarrow 1)$ and (b) $\nu_{12}(J = 1 \rightarrow 2)$ as a function of laser power; the dashed lines are linear fits to the data to extract the zero-power values. A laser power of 350 μW corresponds to an intensity of $\sim$0.45 mW/cm^2 or $\sim$13% of the saturation intensity of 3.4 mW/cm^2.

in power over time. The power fluctuations average out over one scan and contribute only to the statistical fluctuation of the photon counts. Nonlinear least-square fits to the data using a Voigt profile as a fit function yield the respective center frequencies. The Voigt profiles fit all curves well with reduced χ^2 of around one. The residuals plotted in the lower part of Fig. 2 show mainly statistical scattering around zero. The values for the fine structure splittings are obtained from the differences in the center frequencies.

Momentum transfer from the laser light to the atoms changes their transverse velocity distribution. Since this effect depends on the laser frequency, any power imbalance in the two laser beams may result in small asymmetries of the resonance profile that can lead to systematic shifts of the fine structure splitting. To minimize this effect, the laser intensity is chosen to be so low that only a few photons are scattered by each atom while transversing the laser beam. Additionally, the fine structure splitting was measured as a function of the laser power over a range from 25 to 350 μW or about 0.9%–13% of the saturation intensity. The corresponding results are shown in Fig. 3. Each data point is the mean of at least four independent measurements. The error bars are given by the standard error of the independent measurements and correspond well to the error of the individual peak fitting plus the statistical fluctuation of the reference laser frequency of about 20 kHz during one measurement. Overall, the results indeed exhibit a small but noticeable power dependence as indicated by the respective slope of the linear regression to the data. The experimental values for the fine structure
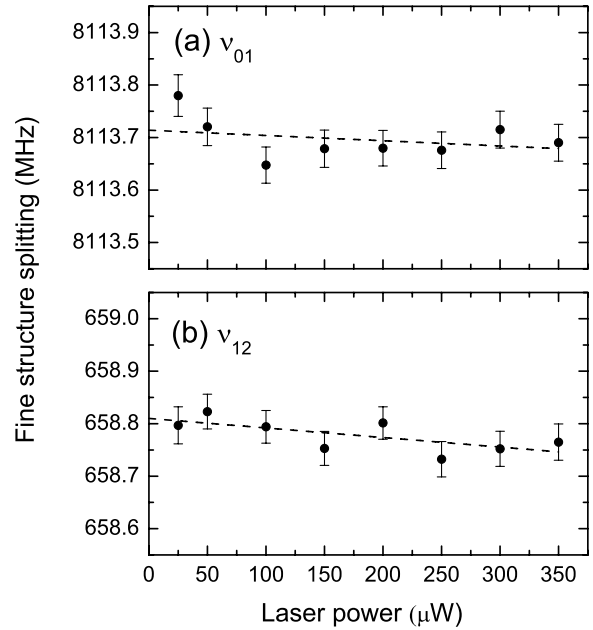
intervals are therefore obtained by extrapolating to zero laser power.

The residual magnetic field within the interaction region was measured to be less than 3 mG. To get an upper estimate for a possible systematic effect caused by this field strength, the magnetic shield was removed and a magnetic field of up to 8 G was deliberately applied. Under these conditions the line center shifted by up to 0.28 MHz/G. Extrapolating this shift to the low field case, we obtain a maximum effect caused by the Zeeman shift of 0.8 kHz, which is negligible at our current level of uncertainty. Systematic effects from light shift and pressure shift are also well below the 1 kHz level. The only remaining effect of importance is systematic laser beam steering. The relative alignment of the counterpropagating laser beams provided by the retroreflecting configuration has a stability of better than 2.5×10^{-3} mrad. The maximum Doppler shift under these conditions is 5 kHz assum-

TABLE II.   Comparison between theoretical and experimental values for the fine structure intervals of the $1s3p\ ^3P_J$ levels in helium. Units are MHz.

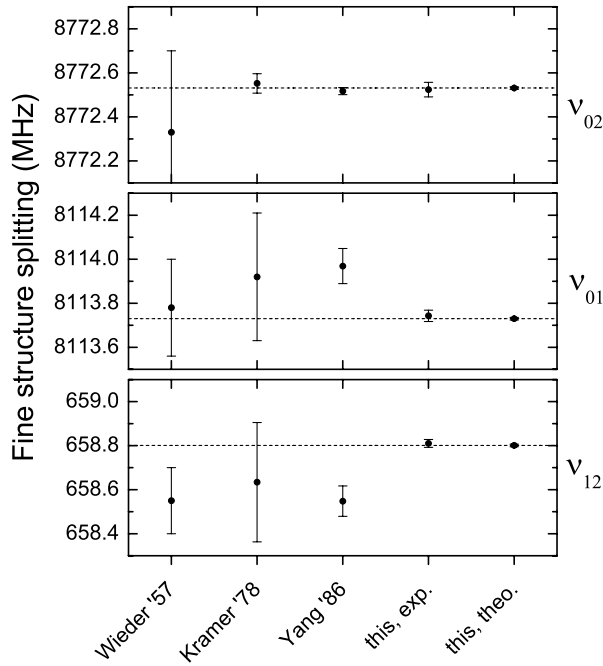| Reference	ν_{01}	ν_{12}	ν_{02}
Wieder [13], exp.	8113.78(22)	658.55(15)	8772.33(37)
Kramer [14], exp.	8113.92(29)	658.63(27)	8772.552(40)
Yang [6], exp.	8113.969(80)	658.548(69)	8772.517(16)
this work, exp.	8113.714(28)	658.810(18)	8772.524(33)
this work, theory	8113.730(6)	658.801(6)	8772.531(6)

FIG. 4.   Comparison of results for the three fine structure intervals of the $1s3p\ ^3P_J$ levels from Wieder *et al.* [13], Kramer *et al.* [14], and Yang *et al.* [6], as well as the experimental and theoretical values from this work. The theoretical values are also indicated by the dashed lines.

ing perpendicular geometry and a helium beam at LN_2 temperature.

The final experimental values for the two independent fine structure intervals $\nu_{01}(J = 0 \rightarrow 1)$ and $\nu_{12}(J = 1 \rightarrow 2)$ with their respective combined statistical and systematic uncertainties are listed in Table II. The results of previously published measurements on all three fine structure intervals of the $1s3p\ ^3P_J$ levels as well as the theoretical and experimental results obtained in this work are compared in Fig. 4.

Our experimental results on the fine structure splittings agree very well with the theoretical calculations. While there is a clear disagreement with the results for the ν_{01} and ν_{12} intervals obtained in [6], the value for ν_{02} of both experiments agrees very well. The previous work was based on the measurement of the magnetic field strength for the crossing point between certain Zeeman sublevels. The extraction of the fine structure splitting values at zero field requires an accurate theoretical analysis of the Zeeman shift [15]. The level crossing of the $J = 0$ and $J = 1$ levels occurs at a considerably higher magnetic field than the $J = 0$ and $J = 2$ crossing. Therefore, the ν_{01} measurement is more sensitive to systematic uncertainties. Since our new experimental approach directly determines the fine structure intervals at zero field, it avoids these complications.

In conclusion, the results from a new experiment measuring the fine structure intervals of the $1s3p\ ^3P_J$ levels in atomic helium resolve an apparent discrepancy between

theory and the previous most precise experimental determination. This provides additional support for the atomic theory calculations of fine structure intervals in atomic helium that serve as the basis for an atomic physics determination of the fine structure constant. For both theory and experiment there is room for improvement. The current limit for theory is the uncertainty in the $B_{5,0}$ QED term, which will receive further attention in the future. On the experimental side, the next step would be a major update of the reference laser to improve its frequency stability, which is currently the dominating source of statistical uncertainties. Additionally, the laser beam coupling into the interaction region needs to be improved to reduce the systematic effect caused by beam steering. Both upgrades should enable measurements down to uncertainties of ~1 kHz. At this level, results from the $1s3p\ ^3P_J$ levels would ideally complement the efforts in improving the $1s2p\ ^3P_J$ data.

*Electronic address: pmueller@anl.gov
†Electronic address: gdrake@uwindsor.ca

[1] G. W. F. Drake, Can. J. Phys. **80**, 1195 (2002).
[2] K. Pachucki and J. Sapirstein, J. Phys. B **35**, 1783 (2002); **35**, 3087 (2002).
[3] M. C. George, L. D. Lombardi, and E. A. Hessels, Phys. Rev. Lett. **87**, 173002 (2001).
[4] J. Castillega, D. Livingston, A. Sanders, and D. Shiner, Phys. Rev. Lett. **84**, 4321 (2000).
[5] F. Minardi, G. Bianchini, P. C. Pastor, G. Giusfredi, F. S. Pavone, and M. Inguscio, Phys. Rev. Lett. **82**, 1112 (1999); P. C. Pastor *et al.*, Phys. Rev. Lett. **92**, 023001 (2004).
[6] D.-H. Yang, P. McNicholl, and H. Metcalf, Phys. Rev. A **33**, 1725 (1986). See Refs. [7,15] for a correction.
[7] F. Marin, F. Minardi, F. S. Pavone, M. Inguscio, and G. W. F. Drake, Z. Phys. D **32**, 285 (1995).
[8] C. S. Adams, E. Riis, A. I. Ferguson, and W. R. C. Rowley, Phys. Rev. A **45**, R2667 (1992).
[9] F. S. Pavone, F. Marin, P. De Natale, M. Inguscio, and F. Biraben, Phys. Rev. Lett. **73**, 42 (1994).
[10] M. Douglas and N. M. Kroll, Ann. Phys. (N.Y.) **82**, 89 (1974).
[11] T. Zhang, Phys. Rev. A **53**, 3896 (1996); T. Zhang and G. W. F. Drake, Phys. Rev. A **54**, 4882 (1996); T. Zhang, Z.-C. Yan, and G. W. F. Drake, Phys. Rev. Lett. **77**, 1715 (1996).
[12] L.-B. Wang, Ph.D. thesis, University of Illinois at Urbana-Champaign, 2004.
[13] I. Wieder and W. E. Lamb, Jr., Phys. Rev. **107**, 125 (1957).
[14] P. B. Kramer and F. M. Pipkin, Phys. Rev. A **18**, 212 (1978).
[15] Z.-C. Yan and G. W. F. Drake, Phys. Rev. A **50**, R1980 (1994).